Reliability-based design of semi-rigidly connected base-isolated buildings subjected to stochastic near-fault excitations

Ali Hadidi, Bahman Farahmand Azar and Amin Rafiee[*]

Department of Civil Engineering, University of Tabriz, Tabriz, Iran

Abstract. Base isolation is a well-established passive strategy for seismic response control of buildings. In this paper, an efficient framework is proposed for reliability-based design optimization (RBDO) of isolated buildings subjected to uncertain earthquakes. The framework uses reduced function evaluations method, as an efficient tool for structural reliability analysis, and an efficient optimization algorithm for optimal structural design. The probability of failure is calculated considering excessive base displacement, superstructure inter-storey drifts, member stress ratios and absolute accelerations of floors of the isolated building as failure events. The behavior of rubber bearing isolators is modeled using nonlinear hysteretic model and the variability of future earthquakes is modeled by applying a probabilistic approach. The effects of pulse component of stochastic near-fault ground motions, fixity-factor of semi-rigid beam-to-column connections, values of isolator parameters, earthquake magnitude and epicentral distance on the performance and safety of semi-rigidly connected base-isolated steel framed buildings are studied. Suitable RBDO examples are solved to illustrate the results of investigations.

Keywords: reduced function evaluations; near-field earthquakes; optimization; base-isolation; rubber bearings; semi-rigid connections

1. Introduction

Nowadays, passive control approaches such as Tuned Mass Damper, Tuned Liquid Damper, Fluid Viscous Damper, Viscoelastic Damper, Friction Damper and Metallic Yield Damper are widely used to improve the seismic performance of structures, due to their cost-effectiveness advantages. Base isolation is also a well-established passive control approach in which a system of isolators provides a flexible base with the structure, thereby, disconnecting the superstructure from the horizontal ground acceleration. In fact, Base isolation improves seismic performance of superstructure by filtering out high frequencies from the ground motion and preventing the building from being damaged. So, it is particularly an effective tool for seismic protection of low- and middle-rise buildings (having high frequencies) (Cheng *et al.* 2008). Application of base isolation to structural systems began in the 1960s (Naeim and Kelly 1999), and up to now, numerous seismically isolated structures have been constructed and many existing buildings have been retrofitted using base isolation technology (Kelly 1986, Mokha *et al.* 1996, Ceccoli *et al.*

∗Corresponding author, Ph.D. Student, E-mail: a.rafiee@tabrizu.ac.ir

1999, DeLuca *et al*. 2001, Chopra 2007, Zou *et al*. 2010, Mazza 2015, Vasiliadis 2016).

As it was stated, base isolation is well-suited for mitigating the vibration effects of earthquakes having high frequencies; hence, excitations with low frequency may have important implications for these structures. In fact, the study of effects of near-fault earthquakes, which frequently include a strong long period pulse, on the performance of structural systems is notable (Jangid and Kelly 2001, Macrae *et al*. 2001, Chopra and Chintanapakdee 2001, Providakis 2008, Cavdar 2013, Jensen and Kusanovic 2014, Domizio *et al*. 2015, Alhan and Ozgur 2015). On the other hand, in the current analysis and design of steel structures, the behavior of beam-to-column connections is assumed to be either perfectly-pinned or fully-rigid; whereas, they are "semi-rigid" in reality. Moreover, different types of connections have different degrees of rigidity. However, they also differ in terms of construction cost (Degertekin and Hayalioglu 2010, Hadidi and Rafiee 2015). Although deterministic design optimization of semi-rigidly connected buildings is available in literature (Hayalioglu and Degertekin 2005, Rafiee *et al*. 2013, Hadidi and Rafiee 2014, Artar and Daloglu 2015), reliability-based design optimization of such structures has not yet been studied. Actual semi-rigid behavior of connections influences directly the period of superstructure and so may has important implications for structures subjected to pulse-like ground motions.

As it was mentioned, in many of studies regarding the optimal design of structures, parameters are considered as deterministic; while, uncertainty exists in their values and therefore these uncertainties should be accounted for by using a reliability-based approach (Juhn and Manolis 1992, Zhang *et al*. 1998, Kawano *et al*. 2002, Alhan and Gavin 2005, Chen *et al*. 2007a, b, Roy and Chakraborty 2013, Mishra *et al*. 2013, Jian *et al*. 2015). Among these uncertainties, those related to stochastic excitation have the most significant effect on the safety of the structure (Jensen and Sepulveda 2012), and should be considered at design stage.

In this paper, an efficient framework for reliability-based design optimization of semi-rigidly connected base-isolated steel buildings subjected to uncertain near-field ground motions is proposed. In this double-loop framework, the recently proposed reduced function evaluations method (Azar *et al*. 2015) is used as an efficient tool for structural reliability analysis; while, the efficient harmony search-based particle swarm optimization (HS-PSO) algorithm (Hadidi and Rafiee 2014) is applied as the optimization technique. Potential variability of future near-fault earthquakes is modeled using point-source probabilistic logic approach (Boore 2003), such that, the uncertainty regarding the future ground motions is properly addressed. Nonlinear hysteretic behavior of rubber bearing isolators is taken into account; whereas, the behavior of superstructure and its connections are assumed to remain at linear range. The first excursion probability o failure is defined as the probability that response quantities of interest (base displacement, superstructure inter-storey drifts, member stress ratios and absolute accelerations of floors, herein) will not exceed allowable limits. Two examples of steel buildings are designed using the proposed methodology. The effects of near-field excitations, semi-rigid connections, different isolator parameters, and earthquake characteristics (moment magnitude and epicentral distance) on the reliability of base-isolated building examples are investigated.

2. Efficient framework for reliability-based design optimization

In this Section, an efficient framework for reliability-based design optimization (RBDO) of structural systems is proposed, which is used in this paper for RBDO of semi-rigidly connected base-isolated steel structures subjected to near-field ground motions. This double-loop framework

uses reduced function evaluations (RFE) method as an efficient tool for solving high-dimensional probability integrals (as inner loop for structural reliability analysis); whereas, search for optimum values for design variables is accomplished by making use of efficient harmony search-based particle swarm optimization (HS-PSO) algorithm (as outer loop for structural optimization).

In the recently proposed RFE method (Azar *et al*. 2015) reliability of a system is analyzed through two main steps: In Initial step, a number of space-filling designs are selected throughout the variables space, and then in Simulation step, performances of most of samples are estimated via interpolation using the space-filling designs, and only for a small number of the samples actual performance function is used for evaluation. In better words, doing so, we use a simple interpolation function called "reduced" function instead of the actual expensive-to-evaluate performance function of the system to evaluate most of samples. By using such a reduced function, total number of evaluations of actual performance is significantly reduced. The RFE has the capability to analyze the reliability of series/parallel systems with multiple failure modes with truncated and/or non-truncated random variables efficiently and accurately. More information about this method can best be found in Azar *et al*. (2015).

Moreover, HS-PSO is a particle swarm optimization (PSO) algorithm (Kennedy and Eberhart 1995) which is improved by hybridizing with harmony search (HS) method (Lee and Geem 2005). It has been shown that the HS-PSO performs better than HS and PSO algorithms (Hadidi and Rafiee 2014). In fact, in HS-PSO algorithm, the harmony memory (HM) is created and improved using particle swarm optimization. On the other hand, the new off-springs generated by PSO, which can be considered as new improvised harmonies, are improved through the concepts used in harmony search. In better words, in HS-PSO the random generation rule, which is used in HS, is removed and instead the PSO is applied, and at the same time, the new position of each bird in the flock is changed by making use of HM consideration rate and pitch adjustment rules. That is to say, we have a swarm of harmonies which flies toward better solutions by adopting the strategy of moving toward the best ever seen position of each bird and that of all birds from PSO, together with the scheme of considering a harmony memory and pitch adjustment from HS. Sufficient details regarding HS, PSO and HS-PSO algorithms can best be found in Hadidi and Rafiee (2014); however, supplementary information on HS and PSO algorithms can be gained in Lee and Geem (2005), Nigdeli *et al*. (2014), Kennedy and Eberhart (1995) and Shi and Eberhart (1998).

3. Semi-rigidly connected seismically-isolated building model

In this study, superstructure (i.e., the structure above the isolation system) is modeled using finite element method, then, static condensation method (Chopra 2007) is applied to the model such that only horizontal translational degree of freedom of each floor, i.e., $u_1, u_2, \cdots u_{nos}$ (*nos* is the number of stories of the planar frame) remains. In this way, number of degrees of freedom of the finite element model is reduced to *nos*, and, the remaining multi-degree-of-freedom system is used as the dynamic model of the building. Structural system modeling is briefly described through following Subsections.

3.1 Semi-rigid beam-to-column connection modeling

Considering the fact that base-isolated buildings are generally designed such that the superstructure remains elastic; here, we model the superstructure as a linear-elastic structural

system. So, the semi-rigid moment-rotation behavior of its beam-to-column connections is modeled as linear. Doing so, a connection is considered to be neither perfectly-pinned nor fully-rigid, and instead, each semi-rigid beam-column member is assumed to be comprised of a finite-length member with a length-less rotational spring attached at each end, as shown in Fig. 1. Hence, a "fixity-factor" for the semi-rigid member can be defined as follows (Monforton and Wu 1963)

$$r_j = \frac{1}{1 + \dfrac{3EI}{R_j L}} \quad (j = 1, 2) \tag{1}$$

where R_j is the end-connection spring stiffness, and EI/L is the flexural stiffness of the attached member. The fixity factor r_j defines the rotational stiffness of each end-connection relative to that of the attached member. For a perfectly-pinned connection, the value of the end-fixity factor is zero ($r_j=0$), and for a fully-rigid connection the end-fixity factor is unity ($r_j=1$). Therefore, a semi-rigid connection has an end-fixity factor between zero and unity ($0<r_j<1$).

3.2 Isolation system modeling

Despite the use of linear-elastic model for the superstructure and its beam-to-column connections, the nonlinear model for the restoring force-deformation behavior of isolation devices is utilized in the present work. Among different base-isolation techniques and devices, rubber bearing isolation system (Kelly 1986, Su *et al*. 1990, Makris and Chang 1998) is considered in this study. This type of device, which consists of layers of rubber vulcanized to the steel plates (Fig. 2), requires less initial and maintenance cost with compared to other control devices. In Fig. 2, D_r and D_i are notations for external and internal diameters of the device, respectively; while, H_r indicates the total height of rubber used in the device.
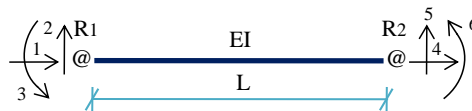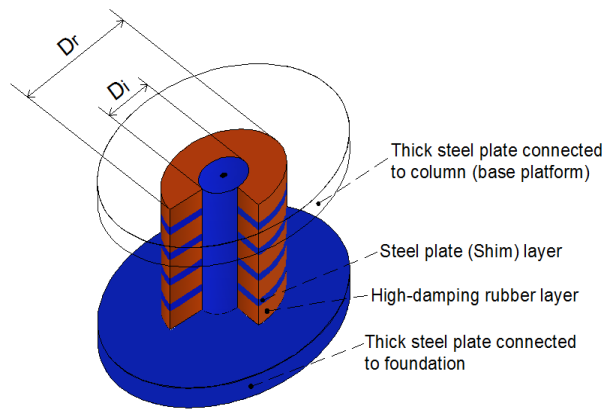

Fig. 1 Semi-rigid member
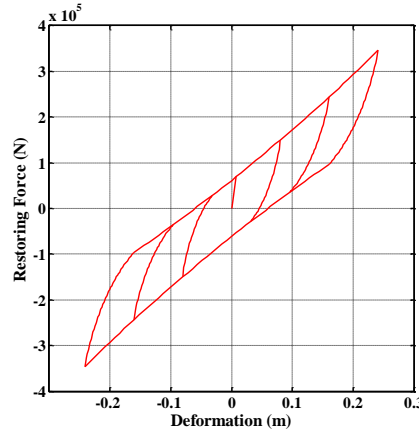

Fig. 2 Rubber bearing device

Fig. 3 Hysteresis loops for rubber bearing with D_r=80 cm, D_i=15 cm and H_r=16 cm

In the present study, the mathematical model used by Jensen and Kusanovic (2014) is utilized for modeling of isolation system. This model which simulates restoring force-deformation of isolation devices has been calibrated using experimental test results conducted for real-size high damping rubber bearings (Yamamoto *et al*. 2009, Minewaki *et al*. 2009). Based on this model, the direction of movement is defined in terms of isolator displacement vector which can be obtained directly from the base displacement (Yamamoto *et al*. 2012, Jensen *et al*. 2012). Then, two components of the restoring force (i.e., the nonlinear elastic and elastoplastic components) are calculated.

According to Yamamoto *et al*. (2012), this simple but accurate model can be used in both unidirectional and bidirectional loading conditions. Fig. 3 shows typical restoring force-deformation loops obtained via mentioned mathematical model for D_r=80 cm, D_i=15 cm and H_r=16 cm, and maximum average shear strains of 50%, 100% and 150%.

3.3 Equation of motion for combined superstructure and isolation system

By applying the procedures described in above Subsections, the mass $\mathbf{M}_s$, damping $\mathbf{C}_s$, and stiffness $\mathbf{K}_s$, matrices of the superstructure can simply be obtained. Also, let $\mathbf{M}_b$, $\mathbf{C}_b$ and $\mathbf{K}_b$ be the corresponding mass, damping and stiffness for the isolation system (base platform). Then, by indicating the vector of relative displacements of the superstructure with respect to the base as $\mathbf{u}_s(t)$ at time instant t, and also by indicating the displacement vector of the base platform as $\mathbf{u}_b(t)$, the dynamic equation of motion of the combined system of superstructure and isolators can be written in the general form of

$$\begin{bmatrix} \mathbf{M}_s & \mathbf{M}_s\mathbf{G}_s \\ \mathbf{G}_s^T\mathbf{M}_s & \mathbf{M}_b+\mathbf{G}_s^T\mathbf{M}_s\mathbf{G}_s \end{bmatrix}\begin{Bmatrix} \ddot{\mathbf{u}}_s(t) \\ \ddot{\mathbf{u}}_b(t) \end{Bmatrix}+\begin{bmatrix} \mathbf{C}_s & \mathbf{O} \\ \mathbf{O} & \mathbf{C}_b \end{bmatrix}\begin{Bmatrix} \dot{\mathbf{u}}_s(t) \\ \dot{\mathbf{u}}_b(t) \end{Bmatrix}+\begin{bmatrix} \mathbf{K}_s & \mathbf{O} \\ \mathbf{O} & \mathbf{K}_b \end{bmatrix}\begin{Bmatrix} \mathbf{u}_s(t) \\ \mathbf{u}_b(t) \end{Bmatrix}=-\begin{bmatrix} \mathbf{M}_s\mathbf{G}_s \\ \mathbf{M}_b+\mathbf{G}_s^T\mathbf{M}_s\mathbf{G}_s \end{bmatrix}\ddot{\mathbf{u}}_g(t)-\begin{Bmatrix} \mathbf{0} \\ \mathbf{f}_{is}(t) \end{Bmatrix} \quad (2)$$

where $\mathbf{G}_s$ is the vector of earthquake influence coefficients of the superstructure corresponding to its degrees of freedom. In addition, $\ddot{\mathbf{u}}_g(t)$ is the horizontal component of ground acceleration (i.e. the stochastic near-fault earthquake in the present study) at time instant t; and, $\mathbf{f}_{is}(t)$ is the nonlinear component of the restoring force induced by isolation devices corresponding to time instant t.

However, it should be noted that the total restoring force of an isolator $\mathbf{f}(t)$, is the sum of two components: a linear component represented by $\mathbf{K}_b\mathbf{u}_b(t)$, and a nonlinear component described by the vector $\mathbf{f}_{is}(t)$ in Eq. (2). It also should be noted that the nonlinear component is calculated in an iterative manner during the dynamic structural analysis of Eq. (2).

4. Stochastic near-fault ground motion model

The existence of uncertainty in the values of various parameters of a structural design problem, and its considerable effect on the performance of a structure, urges designers to take these uncertainties into account. One of the most important sources of uncertainty, which has significant influence, is the uncertainty about the characteristics of future earthquakes. Hence, a probabilistic model for efficiently describing the stochastic excitation, i.e., the ground motion time history, is required in reliability assessment. Since the reliability analysis method used in this paper is simulation-based, it allows for consideration of more complicated descriptions for the ground motion. Here, we use the model developed based on the methodologies presented by Mavroeidis and Papageorgiou (2003) and Boore (2003) (Taflanidis 2007). By applying their methodologies, the low-frequency (long-period) and high-frequency components of the ground motion are independently modeled, and then combined to form the acceleration time history. The procedures for generating high- and low-frequency components are, respectively, described in Subsections 4.1 and 4.2, and finally, the model for generation of near-fault ground motion time history is presented in Subsection 4.3.

4.1 High-frequency component

The point-source stochastic method for modeling of high-frequency component is based on radiation spectrum $A(f;M,r)$ (a frequency-domain function of earthquake magnitude M and epicentral distance r), and envelope function $e(t;M,r)$ (a time-domain function of M and r). The radiation spectrum accounts for the spectral effects from the source (source spectrum) as well as propagation through the earth's crust; whereas, the envelope function addresses the duration of the ground motion. More details about these functions can best be found in Boore (2003).

The high-frequency ground motion time history for an earthquake with specific M and r can simply be obtained through following steps:
(i) Create a white-noise sequence;
(ii) Multiply the white-noise sequence by the envelope function;
(iii) Transform the modified sequence to the frequency domain;
(iv) Now, normalize the sequence by the square root of the mean square of the amplitude spectrum;
(v) Multiply the normalized sequence by the radiation spectrum; and finally,
(vi) Transform the obtained sequence back to the time domain to yield the desired acceleration time history.

4.2 Low-frequency component

As it was stated, near-fault earthquakes frequently include a strong long-period pulse component, for describing the characteristics of such a pulse, the analytical model developed by

Table 1 Parameters for predictive relationships for near-fault pulse characteristics

Soil Condition	Pulse period			PGV				
	a_p	b_p	Standard deviation for ε_f	c_p	d_p	e_p	g_p	Standard deviation for ε_v
Rock	-8.60	1.32	0.40	4.46	7.00	0.34	-0.58	0.39
Soil	-5.60	0.93	0.58	4.58	7.00	0.34	-0.57	0.49
All motions	-6.37	1.03	0.57	4.51	7.00	0.34	-0.57	0.49

Table 2 Random variables of stochastic near-fault ground motion

Variable	Distribution type	Mean value	Standard deviation	Truncation range
γ_p	Normal	1.8	0.3	[1.05, 2.55]
v_p	Uniform	-	-	$[-\pi/2, \pi/2]$
ε_f	Normal	0	0.57	[-1.425, 1.425]
ε_v	Normal	0	0.49	[-1.225, 1.225]

Mavroeidis and Papageorgiou (2003) is chosen. Accordingly, the ground motion velocity pulse is described based on the peak ground velocity (PGV), prevailing frequency (f_p), phase angle (v_p), number of half-cycles (γ_p) and the time shift to specify the epoch of the envelope's peak.

In order to take into account the uncertainties, Bray and Rodriguez-Marek (2004) suggested that the mean values for the logarithms of the pulse period and the peak ground velocity of the ground motion be obtained as

$$\begin{cases} \ln(1/f_p) = a_p + b_p M + \varepsilon_f \\ \ln(PGV) = c_p + e_p M + g_p \ln(r^2 + d_p^2) + \varepsilon_v \end{cases} \tag{3}$$

whose parameter values are given in Table 1, wherein, ε_f and ε_v are prediction errors. It was also suggested by Bray and Rodriguez-Marek (2004) that the prediction errors follow a Gaussian distribution with zero mean and standard deviation that are also presented in Table 1.

4.3 Probabilistic near-fault ground motion model

The acceleration time history for stochastic near-fault earthquake can finally be obtained by combining the above-mentioned components together. The uncertain model parameters are considered in this paper to be the prediction errors of peak ground velocity and prevailing frequency (ε_v and ε_f, respectively), phase angle v_p, and number of half-cycles γ_p; whereas, earthquake magnitude and epicentral distance (M and r) are assumed for simplicity to be deterministic. The mean and standard deviation values of uncertain parameters are given in Table 2. The values of this Table are chosen based on Taflanidis (2007) and Jensen and Kusanovic (2014) with small changes. However, the random variables of the RBDO problem under consideration are not limited to these four truncated variables, and the problem is a high-dimensional one considering the fact that the white-noise sequence has a random variable for each time instant which is uniformly distributed over the range [0, 1].

The following steps describe the model for the probabilistic near-fault earthquake (Mavroeidis

and Papageorgiou 2003):

(i) Apply the stochastic method to generate an acceleration time history (Subsection 4.1);

(ii) Generate a velocity time history for the near-field pulse (Subsection 4.2). The pulse is shifted in time to coincide with the peak of the envelope function. Then, differentiate the velocity time series to obtain an acceleration time series;

(iii) Calculate the Fourier transform of the acceleration time histories generated in above two steps;

(iv) Now, subtract the Fourier amplitude of the time series generated in Step (ii) from the spectrum of the series generated in Step (i);

(v) Construct a synthetic acceleration time history so that its Fourier amplitude is the one calculated in Step (iv) and its Fourier phase coincides with the phase of the time history generated in Step (ii); and finally,

(vi) Superimpose the time histories generated in Steps (ii) and (v).

Fig. 4 depicts a synthetic near-fault ground motion sample for values $M=6.7$, $r=5$ km, $\gamma_p=1.7$, $v_p=\pi/6$, $\varepsilon_v=0$ and $\varepsilon_f=0$.

5. Numerical examples

In this part of the paper, performance and reliability of different examples of semi-rigidly

(a) High-frequency component   (b) Low-frequency pulse component

(c) Final ground motion (velocity time history)   (d) Final ground motion (acceleration time history)
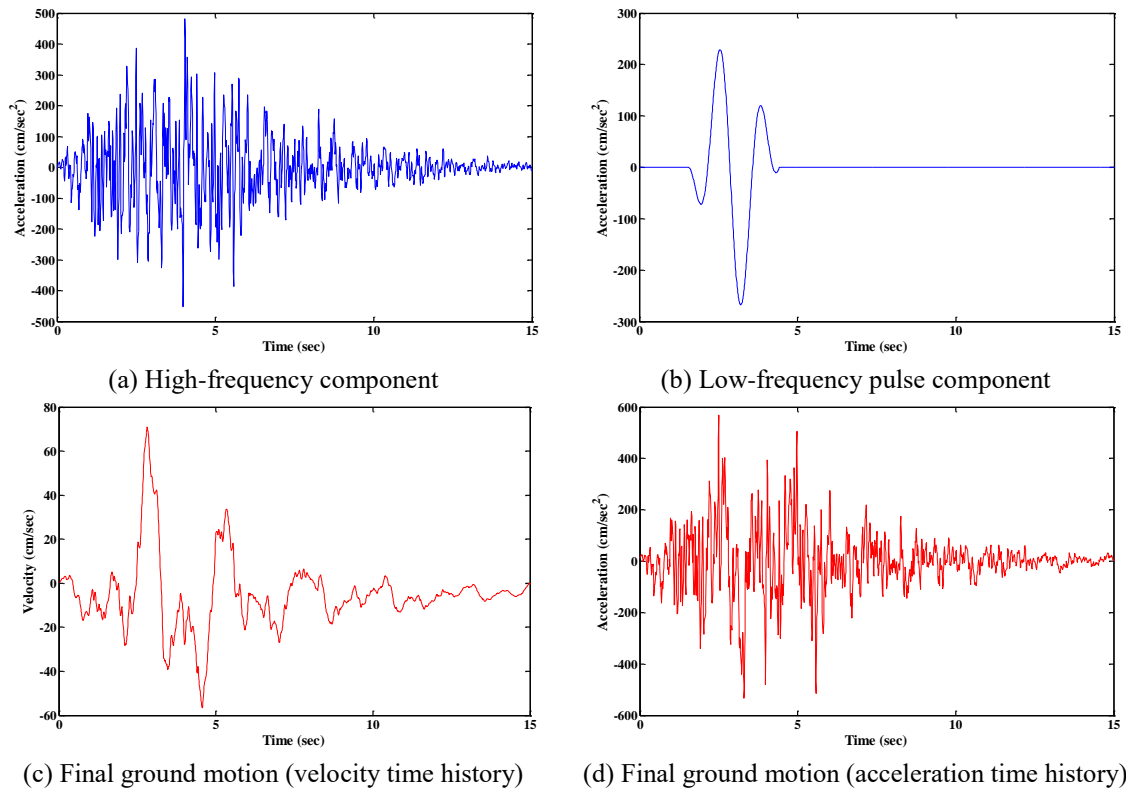
Fig. 4 Sample stochastic near-fault ground motion

connected base-isolated steel moment frames under uncertain near-fault earthquakes are investigated. For this aim, the reliability of a combined system of isolators (base platform) and superstructure is defined as the probability that none of the maximum values of

(i) Displacement of base platform with respect to ground;

(ii) Inter-storey drift of stories of the building;

(iii) Stress calculated based on the interaction of bending and axial forces along the members of the frame; and,

(iv) Absolute acceleration of floors of the building,

will not exceed their allowable bounds during earthquake. So, the performance function for this problem is defined as

$$g(\mathbf{X},\mathbf{D})=1-\max_{i,t}\left(\frac{\left|p_i(t,\mathbf{X},\mathbf{D})\right|}{p_i^*}\right) \quad t\in[0\ T] \tag{4}$$

where, $\mathbf{X}$ and $\mathbf{D}$ are, respectively, the vectors of random and deterministic variables; i is the index which refers to the performance measures defining the limit state. For example, for a planar model of building with *nos* number of stories and *nom* number of members, the maximum i index will be $1+nos+nom+nos$, wherein, the four terms correspond to the four groups of failure events described above. Also, $\left|p_i(t,\mathbf{X},\mathbf{D})\right|$ is the absolute value for the i-th performance measure at time instant t, and p_i^* is its allowable bound. In addition, T is the duration of the earthquake.

Keeping in mind that the $g\leq0$ corresponds to the failure of the structure, the probability of failure of the system can be obtained by solving the multi-dimensional probability integral of

$$P_f(\mathbf{D})=\int_{g(\mathbf{X},\mathbf{D})\leq0}f_{PDF}(\mathbf{X})d\mathbf{X} \tag{5}$$

for a specific $\mathbf{D}$. In this equation, $f_{PDF}(\mathbf{X})$ is the value of joint-probability-density-function for a specific $\mathbf{X}$.

It should be noted that in this paper, AISC-LRFD (2010) specifications is selected as the code of practice for calculating the interaction of bending and axial stresses for members. The strengths of the members are also obtained based on this code.

In the present work, all the dynamic structural analyses, reliability analyses and design optimization are carried out by preparing a home-made computer program. In this program, the HS-PSO algorithm with harmony-memory-consideration-rate of *HMCR*=0.7 and pitch-adjustment-ration of *PAR*=0.4 (as suggested in Hadidi and Rafiee 2014) is used for optimization; while, for reliability analysis the RFE method (with threshold-for-critical-region of TCR=0.45, auto-tuning parameter of ε=0.0002, interpolation power of n=3 and 2000 space-filling-designs (SFDs) produced by making use of low-discrepancy sequences) is used.

5.1 Example 1: A four-storey, two-bay building frame

Consider the unbraced moment-resistant steel frame illustrated in Fig. 5 as an example of building model. As it is seen from this figure, it is a four-storey, two-bay frame with four member groups (i.e., B1 and B2 for beams and C1 and C2 for columns). Fig. 5 also shows the geometry and topology of the frame. The translational degrees of freedom of the floors of the building are $u_1,u_2...u_4$; while, that of base platform is u_b. The building is isolated using three isolation devices. It is assumed that these devices are identical, with same D_i, D_r and H_r.
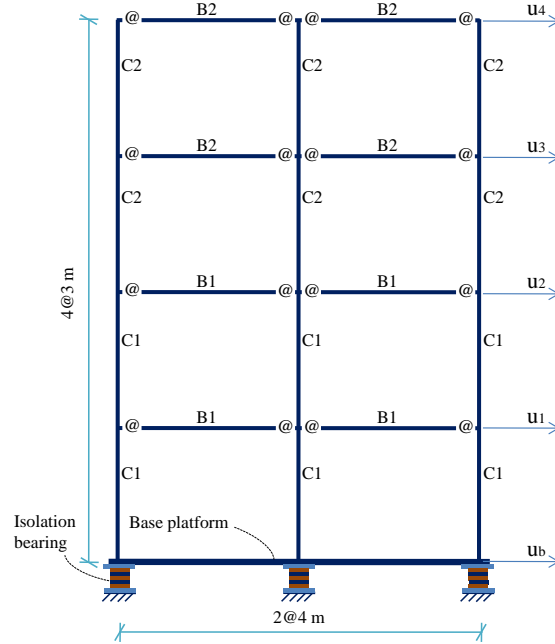
Fig. 5 The four-storey, two-bay frame (Example 1)

Here, the goal of the RBDO problem is to minimize the total cost of the superstructure and isolation system. To this end, the cost of superstructure is simply defined as the total weight of the structural elements (beams and columns); whereas, the cost of isolation system is assumed to be the total volume of the rubber used in the devices. Hence, the problem can be formulated as follows

$$
\begin{aligned}
Minimize \quad & \left\{ Weight\left(B1,B2,C1,C2\right),\ Volume\left(D_r,H_r\right) \right\} \\
Subjected\ to \quad & P_f\left(B1,B2,C1,C2,\ D_r,H_r\right) \leq P_f^* \\
& D_r \in \left\{ 30,35,40,45,50,55,60 \right\} cm \\
& H_r \in \left\{ 15,17,19,21,23,25 \right\} cm \\
B1,B2,C1,C2 \in & \left\{ W12,W14,W16,W18,W21,W24 \right\} AISC\ Wide-flange\ sections
\end{aligned}
\tag{6}
$$

where, $P_f^* = 0.025$ is allowable probability of failure of the combined system of isolators and superstructure. This problem is multi-objective in nature; however, we use a single objective as

$$
Cost\left(B1,B2,C1,C2,\ D_r,H_r\right) = Weight\left(B1,B2,C1,C2\right) \times \left[\frac{Volume\left(D_r,H_r\right)}{Volume\left(D_r^{\min},H_r^{\min}\right)} \right]
\tag{7}
$$

instead, wherein, $D_r^{\min}$ and $H_r^{\min}$ are the minimum allowable values for D_r and H_r (30 cm and 15 cm, herein), respectively. The problem defined in Eq. (6) has six discrete design variables i.e., $B1$, $B2$, $C1$, $C2$, D_r, H_r. The P_f is calculated based on the four groups of failure events presented in Eq. (4) with allowable base displacement of 30 cm and allowable absolute floor acceleration of $0.35g$ (g is the gravitational acceleration). This acceleration limit is suitable for structural integrity;

however, a comprehensive discussion on practical limits of floor accelerations in base-isolated buildings can best be found in the valuable work of Alhan and Davas (2016). Also, allowable bounds for member stresses and inter-storey drifts are chosen based on AISC-LRFD (2010) specifications. In addition to the random variables involved in white-noise sequence, the four random variables of this problem are given in Table 2, and the other parameters are considered to be deterministic. The earthquake magnitude and epicentral distance values are fixed at M=6.4 and r=20 km, respectively. The mass values of all floors are assumed to be equal to that of base platform m_b=21.98 ton. Modal damping of the superstructure is taken as 5%. The modulus of elasticity and yield stress for the steel material is 200 GPa and 248 MPa, respectively. For rubber bearings the D_i is fixed at 15 cm and the fixity-factor for both ends of all the semi-rigidly connected beam members are assumed to be equal to 0.7.

In order to solve this problem, the constrained optimization problem is transformed into an unconstrained one by making use of following penalty function

$$\varphi\left(B1, B2, C1, C2, D_r, H_r\right) = 1 + \max\left\{0, \ 100 \times \left(P_f - P_f^*\right), \ 10 \times \left[\sum_{p=1}^{nj}\max\left\{0, V_p\right\} + \sum_{q=1}^{nc}\max\left\{0, V_q\right\}\right]\right\} \quad (8)$$

where V_p and V_q refers to the other group of constraints imposed on the optimization problem, which arises from the size adaptations of beams and columns relative to each other. This group consists of two constructional considerations: one consideration implies that flange width of a beam must be smaller than the same value for column in all joints; whereas, the other one considers the fact that the column of each storey cannot be smaller in depth compared to its above storey column. These two constraints can be formulated, respectively, as

$$V_p = \frac{b_f^{bp}}{b_f^{cp}} - 1.0, \quad p = 1, 2, \ldots nj \quad (9)$$

$$V_q = \frac{d_c^{uq}}{d_c^{lq}} - 1.0, \quad q = 1, 2, \ldots nc \quad (10)$$

where b_f^{bp} and b_f^{cp} are the value of flange width for beam and column in node number p among the total number of nj nodes, respectively (nj is the total number of nodes of frame except the supports). The d_c^{uq} and d_c^{lq} are notations for depths of column sections of upper and lower floor in a node, respectively. nc is the total number of columns in the frame excluding ones for first storey. Finally, the Cost function of Eq. (7) is multiplied by the penalty function of Eq. (8) to give the final unconstrained objective function.

The result of the RBDO problem is given in Table 3. For beam and column sections fixed at those reported in this table, the iso-probability-of-failure (shown in red) and iso-cost (shown in blue) sets of curves for different values of D_r and H_r are depicted in Fig. 6. The design space in this problem is discrete; however, this figure is obtained by calculating failure probability for additional values of D_r and H_r. Also, it should be noted that in this figure the iso-cost curves are drawn for the normalized volume of the isolators (i.e., the term within brackets in Eq. (7)). As it is seen from this figure, the feasible domain has two designs, one of them is the optimum listed in Table 3, and the other is the design with D_r=40 cm and H_r=23 cm with P_f=0.0245 which locates on the iso-cost curve of 3.12 (i.e., the total cost of 12,866 kg).

Table 3 Results of the RBDO problem (Example 1)

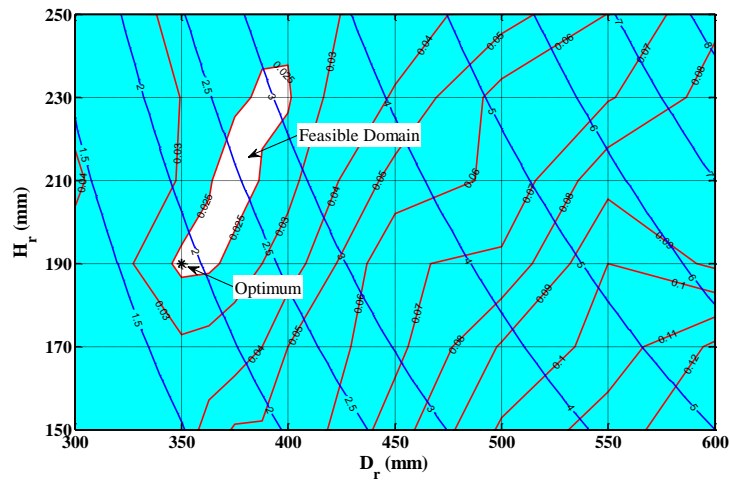| Design variable	Optimum value
$B1$	W14×22
$B2$	W12×14
$C1$	W12×87
$C2$	W12×35
H_r (mm)	190
D_r (mm)	350
Probability of failure	0.0238
Superstructure weight (kg)	4,120
Total cost (kg)	7,732

Fig. 6 Design space for the RBDO problem of Example 1

Now, the effect of fixity-factor of semi-rigidly connected members on the reliability of the optimum design subjected to near-fault earthquake is investigated. For this aim, we keep all the variables fixed at foregoing values and at those reported in Table 3, and only change the fixity-factor which was 0.7 up to now. For different values of end fixity factors equal to 0.4, 0.5 … 1.0, Fig. 7 shows the failure probability. As it is seen from the results, the increase in the fixity-factor decreases the failure probability of the base-isolated building. However, this decrease itself is on the decrease as the fixity-factor goes toward unity (fully-rigid connection). On the other hand, it is noteworthy that the construction cost of a beam-to-column connection increases as its degree of rigidity (i.e., the fixity-factor) increases (Hadidi and Rafiee 2015). So, the selection of a suitable beam-to-column connection in a base-isolated steel building will result in a cost-effective and/or reliable design of such a structure.

Let us investigate now the effects of fixity-factor and near-fault earthquake in more details. Keeping again all the variables fixed at foregoing values and at those reported in Table 3, and for end fixity factors of 0.4 and 1.0, Fig. 8 shows the base displacement response of the isolated building subjected to a sample of far-field (having high-frequency component only) and near-field

(with pulse component) earthquake. As it is seen from the results, the end fixity factor has not considerable effect on the base displacement; whereas, the pulse component included in near-fault ground motion significantly increases the horizontal displacement of the base platform.
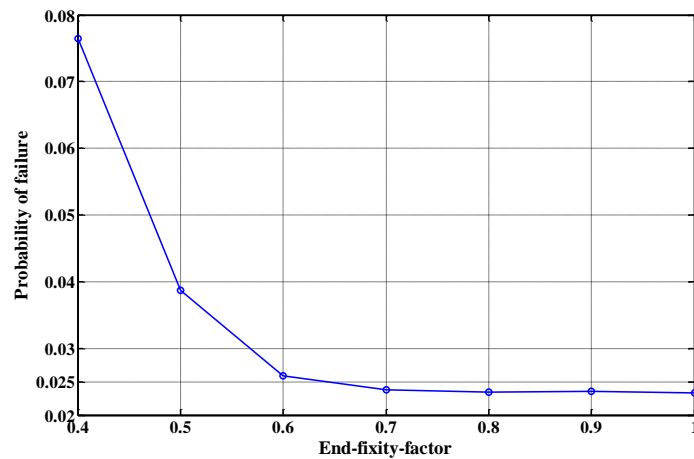

Fig. 7 Failure probability of semi-rigidly connected base-isolated building for different end fixity factors

(a) Far-field earthquake (fixity-factor=0.4)

(b) Near-field earthquake (fixity-factor=0.4)

(c) Far-field earthquake (fixity-factor=1.0)

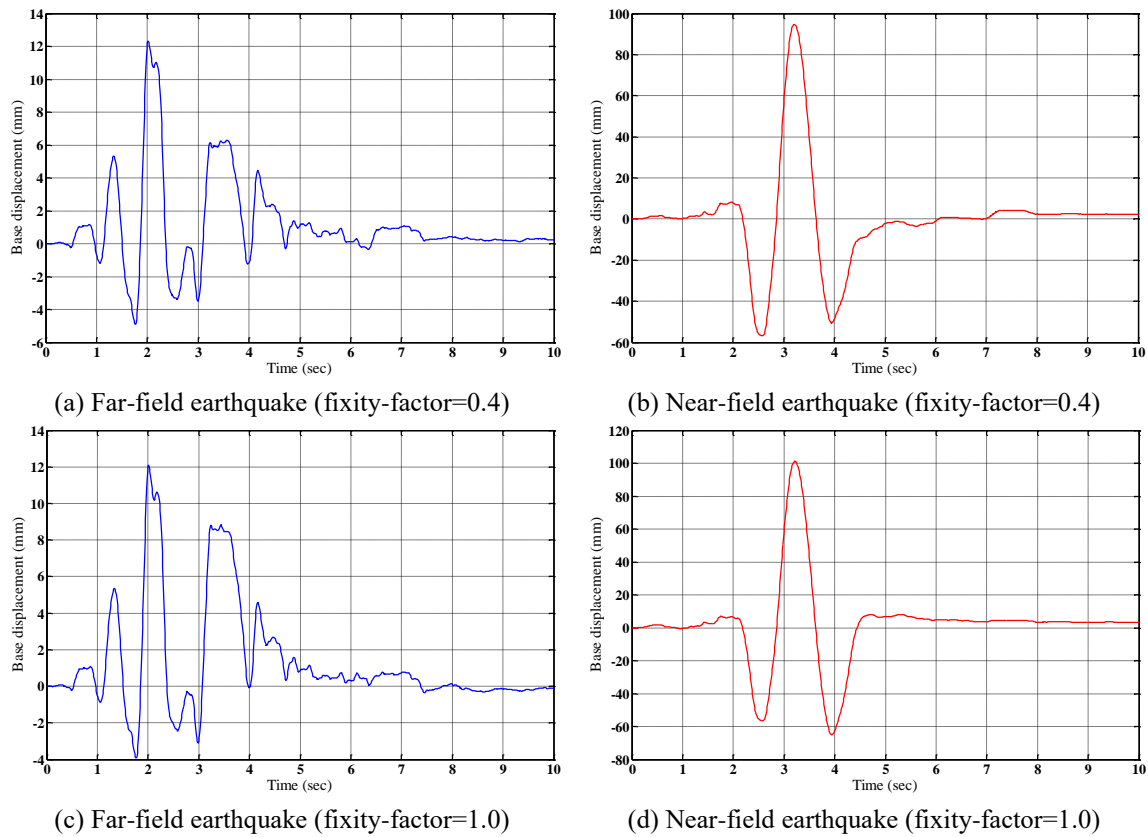(d) Near-field earthquake (fixity-factor=1.0)

Fig. 8 Horizontal displacement response of the base platform

On contrary to the effect of end fixity factor on the base displacement response, the horizontal displacement response of the roof level of the isolated building with respect to base is significantly affected by fixity-factor of end connections of semi-rigid structural elements. This effect can be seen from Fig. 9, wherein, the roof displacement of isolated building is depicted for fixity factors of 0.4 and 1.0 subjected to far- and near-field excitations. As it is seen, pulse component increases the roof displacement; however, this increase itself increases as the fixity-factor of beam-to-column connections decreases. Furthermore, the decrease in fixity-factor is accompanied by increase in roof displacement (compare Figs. 9(a) with 9(c), and, 9(b) with 9(d)). In better words, the decrease in fixity-factor is accompanied by increase in roof displacement; but, this increase is more significant when the earthquake includes strong long-period pulse component which frequently occurs in near-fault regions.

On the other hand, the roof displacement of fixed-base building is also increases with the decrease in fixity-factor, but at a rate slower than that of isolated-building. That is to say, the effectiveness of base-isolation in decreasing the roof displacement is less for buildings with very flexible connections. To show this, the roof displacement of base-isolated building is compared with that of fixed-base building for three cases with fixity factors of 0.4, 0.7 and 1.0 subjected to near-fault earthquake. The results are shown in Figs. 10(a)-(c), wherein, the maximum roof displacement of isolated building is reduced to 82%, 55% and 43% of that of fixed-base building,
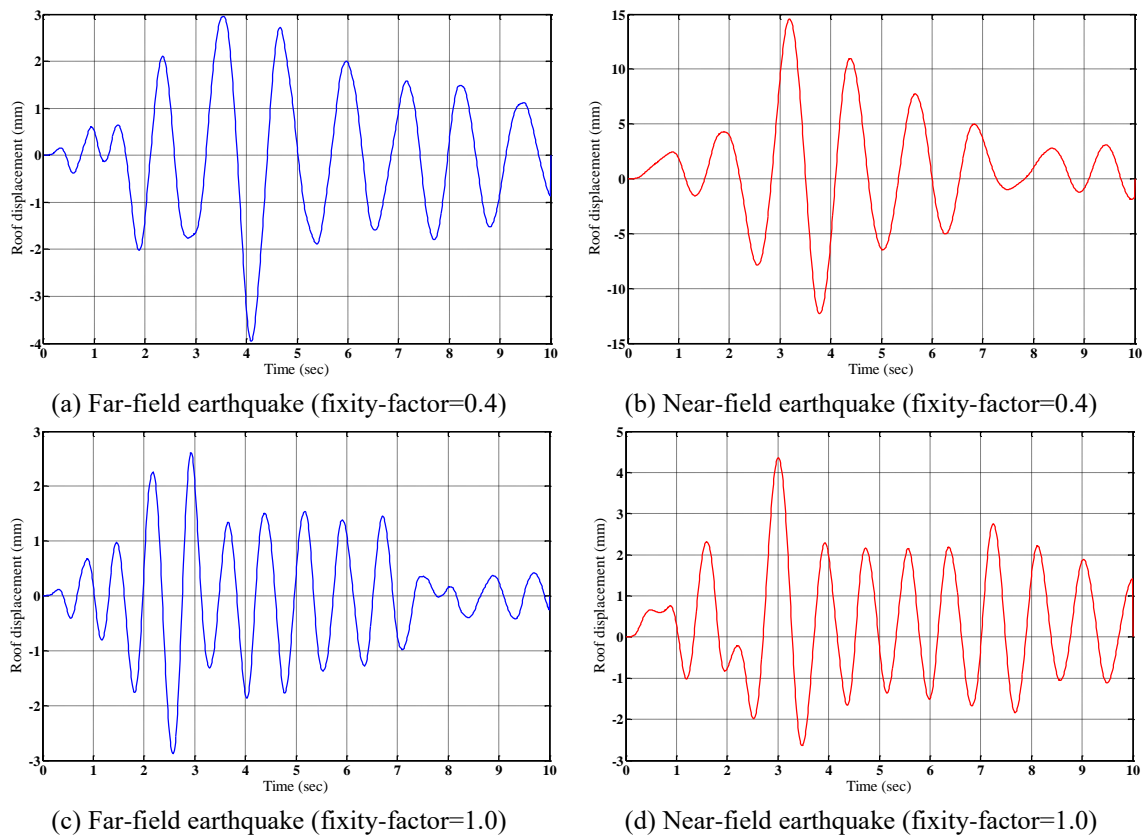

(a) Far-field earthquake (fixity-factor=0.4)

(b) Near-field earthquake (fixity-factor=0.4)

(c) Far-field earthquake (fixity-factor=1.0)

(d) Near-field earthquake (fixity-factor=1.0)

Fig. 9 Horizontal displacement response of the roof level with respect to base

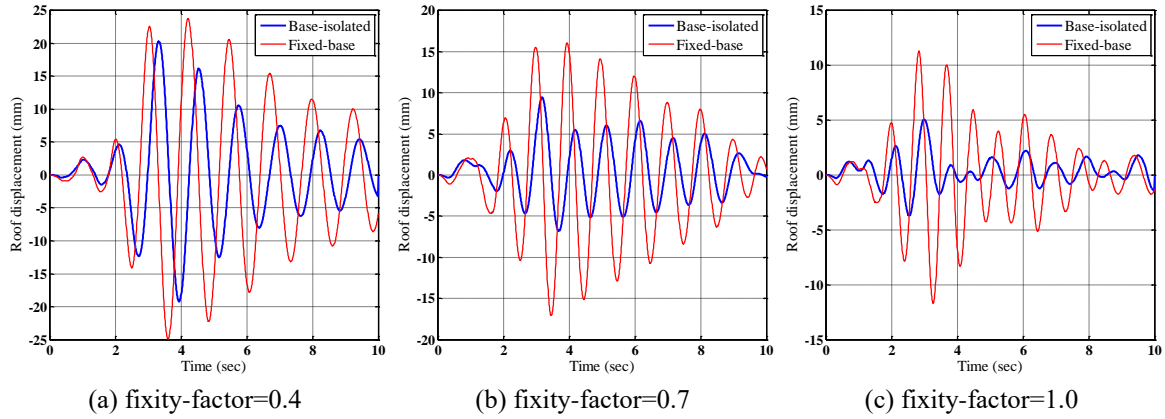(a) fixity-factor=0.4   (b) fixity-factor=0.7   (c) fixity-factor=1.0

Fig. 10 Roof displacement of building with respect to base subjected to near-fault ground motion
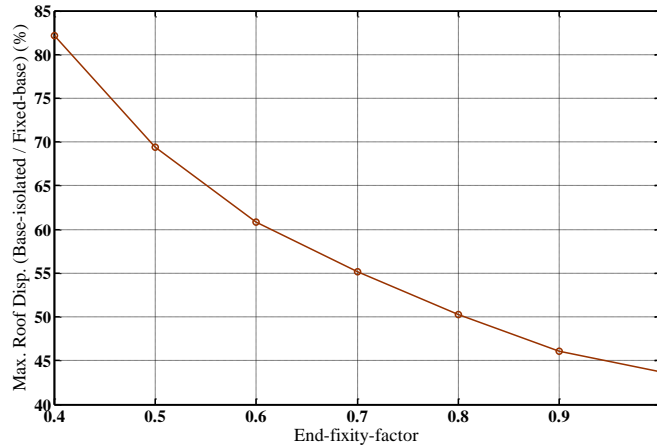

Fig. 11 Effectiveness of base-isolation in decreasing maximum roof displacement

respectively. For 50 samples of stochastic near-fault excitation, these percentages are calculated and the mean values of them are reported for different fixity factors in Fig. 11. It is clear from this figure that the effectiveness of base-isolation in decreasing the roof displacement, decreases with the decrease in fixity-factor.

5.2 Example 2: A four-storey, four-bay building frame

As another example, the RBDO of a steel moment frame with 4 stories and 4 bays is studied. Fig. 12 shows the geometry, topology and member grouping (B1, B2, C1 and C2) for this frame. As shown in this figure, the frame is similar to the frame of Example 1 except the number of bays is increased from 2 to 4 while the length of each span has been reduced from 4 m to 3 m. Analogously, the translational degrees of freedom of the floors of the building are $u_1, u_2 \ldots u_4$, while that of base platform is u_b. The isolation system of the building is equipped with 5 rubber bearing devices. As done for previous example, it is assumed that these devices are identical in terms of D_i, D_r and H_r.
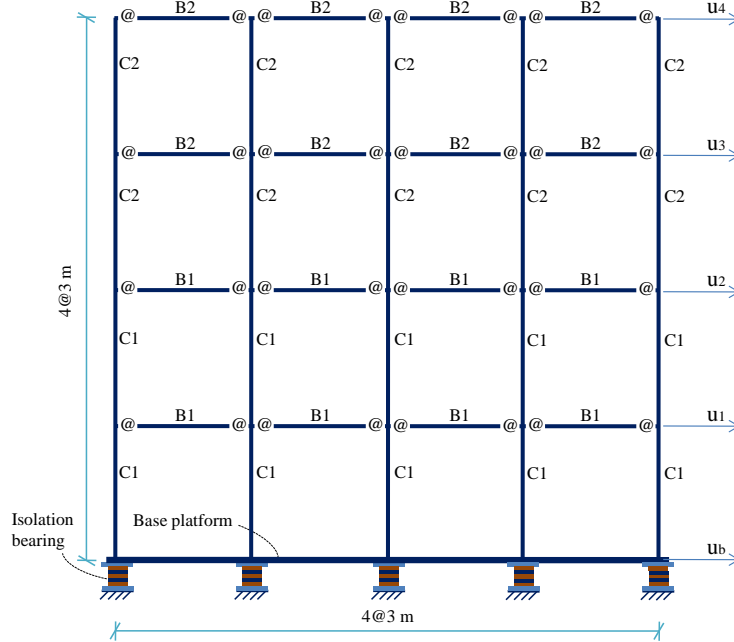
Fig. 12 The four-storey, four-bay frame (Example 2)

The goal of this example is to design the superstructure and its isolation system with the minimum probability of failure, while, the total weight of structural elements (beams and columns) is limited to a predetermined target value. This reliability maximization problem is formulated as

$$\begin{aligned}
&Minimize \quad P_f\left(B1, B2, C1, C2,\ D_r, H_r\right) \\
&Subjected\ to \quad Weight\left(B1, B2, C1, C2\right) \le W^* \\
&\qquad\qquad 40 \le D_r \le 70\ cm \\
&\qquad\qquad 15 \le H_r \le 25\ cm \\
&B1, B2, C1, C2 \in \left\{W12, W14, W16, W18, W21, W24\right\} AISC\ Wide-flange\ sections
\end{aligned}$$
(11)

where, W^*=20,000 kg is the target structural weight. This problem has two continuous (i.e., D_r, H_r) and four discrete (i.e., $B1$, $B2$, $C1$, $C2$) design variables.

In calculating the P_f on the basis of failure events described in Eq. (4), the allowable values for base displacement and absolute floor acceleration are considered to be 40 cm and 0.4×gravitational acceleration, respectively. AISC-LRFD (2010) code is also used to determine the allowable bounds for member stresses and inter-storey drifts. The random variables of this problem are those needed for white-noise sequence and those listed in Table 2, and the other parameters are deterministic. In this example, the earthquake magnitude and epicentral distance are M=6.8 and r=15 km. The mass of each floor is equal to 87.92 ton; whereas, mass of base platform is 123.09 ton. The values of modal damping of the superstructure, D_i of rubber bearings, end-fixity-factor of semi-rigidly connected members and mechanical properties of the steel material are the same values used in previous example.

Analogous to previous example, the constrained optimization problem is transformed into an

unconstrained one by making use of penalty function which is in this case as follows

$$\varphi\left(B1,B2,C1,C2\right)=1+10\times\left[\max\left\{0,\left(\frac{W-W^*}{W^*}\right)\right\}+\sum_{p=1}^{nj}\max\left\{0,V_p\right\}+\sum_{q=1}^{nc}\max\left\{0,V_q\right\}\right] \tag{12}$$

where V_p and V_q have been previously described in Eqs. (8)-(10), which arises from the size adaptations of structural elements. W is the same *Weight* ($B1$, $B2$, $C1$, $C2$) function and W^* is its target value. At last, the final unconstrained objective function is constructed by multiplying the P_f function in Eq. (11) by the penalty function of Eq. (12). Table 4 presents the result of this reliability maximization problem.

Now, let us examine the effects of fixity-factor of semi-rigidly connected members and near-fault earthquake characteristics on the reliability of the optimum design. For this purpose, we fix the values of all the variables at foregoing values and at those reported in Table 4, except the fixity-factor, earthquake magnitude and epicentral distance which were 0.7, 6.8 and 15 km prior to this. For different values of these parameters, Figs. 13(a)-(c) show the failure probability. As it is seen from the results, in general, the increase in the fixity-factor decreases the failure probability of the base-isolated building. However, as it was the case for previous example, this decrease itself is on the decrease as the fixity-factor goes toward unity (fully-rigid connection). Nevertheless,

Table 4 Results of the RBDO problem (Example 2)

Design variable	Optimum value
$B1$	W12×16
$B2$	W14×43
$C1$	W18×65
$C2$	W14×159
H_r (mm)	226.55
D_r (mm)	518.23
Probability of failure	0.0618
Superstructure weight (kg)	12,127

(a) Epicentral distance=5 km   (b) Epicentral distance=15 km   (c) Epicentral distance=25 km
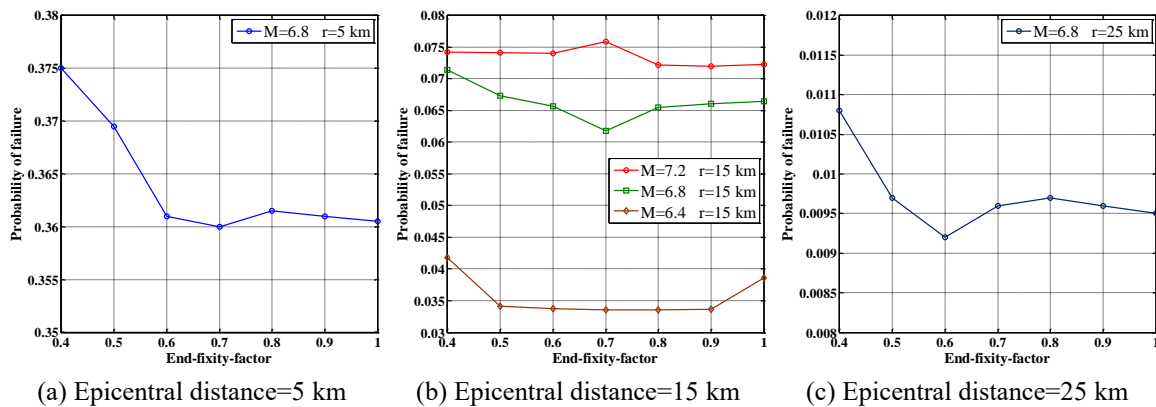
Fig. 13 Failure probability of semi-rigidly connected base-isolated building for different end fixity factors

there are some irregularities and this trend does not hold in all cases. Considering again the fact that the construction cost of a beam-to-column connection increases as its degree of rigidity (i.e., the fixity-factor) increases, it is emphasized once again that by selecting suitable beam-to-column connections for base-isolated steel buildings the construction cost and/or failure probability of these structures can be minimized.

Moreover, the results show that the probability of failure of combined system of isolators and superstructure is very sensitive to epicentral distance. Additionally, the sensitivity of failure probability with respect to earthquake magnitude is high for small values of M and decreases as the M increases (compare P_f of the case 6.4 with 6.8, and the case 6.8 with 7.2 in Fig. 13(b)).

6. Conclusions

An efficient framework for reliability-based design optimization of base-isolated buildings with semi-rigid beam-to-column connections subjected to uncertain near-fault earthquakes was proposed. The framework uses reduced function evaluations method for calculating failure probability of the structure; while, harmony search based particle swarm optimizer is used as the optimization tool in the proposed framework. Excessive base displacement, superstructure inter-storey drifts, member stress ratios and absolute accelerations of floors were considered as failure events defining the limit-state. The behavior of rubber bearing isolators was modeled using nonlinear hysteretic model and the variability of future earthquakes was modeled by applying a probabilistic approach. Suitable design examples were solved to study the effects of stochastic pulse component of near-fault ground motions, fixity factors of ends of semi-rigidly connected elements, rubber bearing isolator parameters, earthquake magnitude and epicentral distance on the performance and reliability of semi-rigidly connected base-isolated steel framed buildings.

The results of these investigations can be summarized as follows:

• Excluding the observed exceptions, in general, the increase in the fixity-factor of ends of semi-rigidly connected members decreases the failure probability of the base-isolated building subjected to near-fault earthquake. However, this decrease itself is on the decrease as the fixity-factor goes toward unity (fully-rigid connection).

• The end fixity factor has not considerable effect on the horizontal displacement of the base platform; whereas, the pulse component included in near-fault ground motion significantly increases the base displacement.

• The decrease in fixity-factor is accompanied by increase in roof displacement of isolated building with respect to base platform; however, this increase is more significant when the earthquake includes strong long-period pulse component which frequently occurs in near-fault regions.

• The effectiveness of base-isolation in decreasing the roof displacement of building with respect to base is less for buildings with very flexible connections, when the earthquake includes pulse component.

• The probability of failure of combined system of isolators and superstructure is very sensitive to epicentral distance of a near-fault earthquake.

• Additionally, the sensitivity of failure probability with respect to earthquake magnitude (M) is high for small values of M, and decreases as the M increases.

• Finally, the selection of suitable beam-to-column connections for a base-isolated steel building will result in a cost-effective and/or reliable design of such a structure. On the other hand,

the sensitivity of results to connection rotational stiffness implies that in retrofitting of existing building with base-isolation, the actual semi-rigid behavior of connections should be taken into account.

However, it should be noted that the abovementioned conclusions were solely concluded for the case of rubber-based isolation systems and more work is required for friction-based isolators. Moreover, the effects of eccentricity, 3D modeling, biaxial interaction of isolators and randomness in the superstructure were not accounted for in the investigations.

References

AISC (2010), *Specification for structural steel buildings*, American Institute of Steel Construction, ANSI/AISC 360-10, Chicago, USA.

Alhan, C. and Davas, S.O. (2016), "Performance limits of seismically isolated buildings under near-field earthquakes", *Eng. Struct.*, **116**, 83-94.

Alhan, C. and Gavin, H.P. (2005), "Reliability of base isolation for the protection of critical equipment from earthquake hazards", *Eng. Struct.*, **27**(9), 1435-1449.

Alhan, C. and Ozgur, M. (2015), "Seismic responses of base-isolated buildings: efficacy of equivalent linear modeling under near-fault earthquakes", *Smart Struct. Syst.*, **15**(6), 1439-1461.

Artar, M. and Daloglu, A.T. (2015), "Optimum design of steel frames with semi-rigid connections and composite beams", *Struct. Eng. Mech.*, **55**(2), 299-313.

Azar, B.F., Hadidi, A. and Rafiee, A. (2015), "An efficient simulation method for reliability analysis of systems with expensive-to-evaluate performance functions", *Struct. Eng. Mech.*, **55**(5), 979-999.

Boore, D.M. (2003), "Simulation of ground motion using the stochastic method", *Pure. Appl. Geophys.*, **160**(3-4), 635-676.

Bray, J.D. and Rodriguez-Marek, A. (2004), "Characterization of forward-directivity ground motions in the near-fault region", *Soil. Dyn. Earthq. Eng.*, **24**(11), 815-828.

Cavdar, O. (2013), "Probabilistic sensitivity analysis of suspension bridges to near-fault ground motion", *Steel Compos. Struct.*, **15**(1), 15-39.

Ceccoli, C., Mazzotti, C. and Savoia, M. (1999), "Non-linear seismic analysis of base-isolated RC frame structures", *Earthq. Eng. Struct. Dyn.*, **28**(6), 633-653.

Chen, S.H., Song, M. and Chen, Y.D. (2007), "Robustness analysis of responses of vibration control structures with uncertain parameters using interval algorithm", *Struct. Saf.*, **29**(2), 94-111.

Chen, J., Weiqing, L., Peng, Y. and Li, J. (2007), "Stochastic seismic response and reliability analysis of base-isolated structures", *J. Earthq. Eng.*, **11**(6), 903-924.

Cheng, F.Y., Jiang, H. and Lou, K. (2008), *Smart Structures: Innovative Systems for Seismic Response Control*, CRC Press, New York, NY, USA.

Chopra, A.K. (2007), *Dynamics of Structures: Theory and Applications to Earthquake Engineering*, (3rd Edition), Prentice Hall, New Jersey, NJ, USA.

Chopra, A.K. and Chintanapakdee, C. (2001), "Comparing response of SDF systems to near-fault earthquake motions in the context of spectral regions", *Earthq. Eng. Struct. Dyn.*, **30**(12), 1769-1789.

Degertekin, S.O. and Hayalioglu, M.S. (2010), "Harmony search algorithm for minimum cost design of steel frames with semi-rigid connections and column bases", *Struct. Multidisc. Optim.*, **42**(5),755-768.

DeLuca, A., Mele, E., Molina, J., Verzeletti, G. and Pinto, A.V. (2001), "Base isolation for retrofitting historic buildings: evaluation of seismic performance through experimental investigation", *Earthq. Eng. Struct. Dyn.*, **30**(8), 1125-1145.

Domizio, M., Ambrosini, D. and Curadelli, O. (2015), "Performance of TMDs on nonlinear structures subjected to near-fault earthquakes", *Smart Struct. Syst.*, **16**(4), 725-742.

Hadidi, A. and Rafiee, A. (2014), "Harmony search based, improved particle swarm optimizer for minimum cost design of semi-rigid steel frames", *Struct. Eng. Mech.*, **50**(3), 323-347.

Hadidi, A. and Rafiee, A. (2015), "A new hybrid algorithm for simultaneous size and semi-rigid connection type optimization of steel frames", *Int. J. Steel Struct.*, **15**(1), 89-102.

Hayalioglu, M.S. and Degertekin, S.O. (2005), "Minimum cost design of steel frames with semi-rigid connections and column bases via genetic optimization", *Comput. Struct.*, **83**(21-22), 1849-1863.

Jangid, R.S. and Kelly, J.M. (2001), "Base isolation for near-fault motions", *Earthq. Eng. Struct. Dyn.*, **30**(5), 691-707.

Jensen, H.A. and Kusanovic, D.S. (2014), "On the effect of near-field excitations on the reliability-based performance and design of base-isolated structures", *Probab. Eng. Mech.*, **36**(2), 28-44.

Jensen, H.A., Kusanovic, D.S. and Papadrakakis, M. (2012), "Reliability-based characterization of base-isolated structural systems", *Proceedings of European Congress on Computational Methods in Applied Sciences and Engineering*, ECCOMAS 2012, Vienna, Austria, September.

Jensen, H.A. and Sepulveda, J.G. (2012), "On the reliability-based design of structures including passive energy dissipation systems", *Struct. Saf.*, **34**(1), 390-400.

Jian, F., Xiaohong, L. and Yanping, Z. (2015), "Optimum design of lead-rubber bearing system with uncertainty parameters", *Struct. Eng. Mech.*, **56**(6), 959-982.

Juhn, G. and Manolis, G.D. (1992), "Stochastic sensitivity and uncertainty of secondary systems in base-isolated structures", *J. Sound. Vib.*, **159**(2), 207-222.

Kawano, K., Arakawa, K., Thwe, M. and Venkastaramana, K. (2002), "Seismic response evaluation of base-isolated structures with uncertainties", *Proceedings of the Second International Conference on Structural Stability and Dynamics*, Singapore, December.

Kelly, J.M. (1986), "Aseismic base isolation: review and bibliography", *Soil. Dyn. Earthq. Eng.*, **5**(4), 202-216.

Kennedy, J. and Eberhart, R. (1995), "Particle swarm optimization", *Proceedings of the IEEE International Conference Neural Networks*, Perth, Australia, **IV**, 1942-1948.

Lee, K.S. and Geem, Z.W. (2005), "A new meta-heuristic algorithm for continuous engineering optimization: harmony search theory and practice", *Comput. Meth. Appl. Mech. Eng.*, **194**(36-38), 3902-3933.

Macrae, G.A., Morrow, D.V. and Roeder, C.W. (2001), "Near-fault ground motions effects on simple structures", *J. Struct. Eng.*, ASCE, **127**(9), 996-1004.

Makris, N. and Chang, S. (1998), Effects of damping mechanisms on the response of seismically isolated structures. PEER Report 1998/06, Berkeley (CA): Pacific Earthquake Engineering Research Center, College of Engineering, University of California.

Mavroeidis, G.P. and Papageorgiou, A.S. (2003), "A mathematical representation of near-fault ground motions", *Bull. Seismol. Soc. Am.*, **93**(3), 1099-1131.

Mazza, F. (2015), "Comparative study of the seismic response of RC framed buildings retrofitted using modern techniques", *Earthq. Struct.*, **9**(1), 29-48.

Minewaki, S., Yamamoto, M., Higashino, M., Hamaguchi, H., Kyuke, H., Sone, T. and Wada, A. (2009), "Performance tests of full size isolators for super high-rise isolated buildings", *J. Struct. Eng. AIJ*, **55**(B), 469-477.

Mishra, S.K., Roy, B.K. and Chakraborty, S. (2013), "Reliability-based-design-optimization of base isolated buildings considering stochastic system parameters subjected to random earthquakes", *Int. J. Mech. Sci.*, **75**, 123-133.

Mokha, A.S., Amin, N., Constantinou, M.C. and Zayas, V. (1996), "Seismic isolation retrofit of large historic building", *J. Struct. Eng.*, ASCE, **122**(3), 298-308.

Monforton, G.R. and Wu, T.S. (1963), "Matrix analysis of semi-rigidly connected frames", *J. Struct. Eng.*, ASCE, **89**(6), 13-42.

Naeim, F. and Kelly, J.M. (1999), *Design of Seismic Isolated Structures: From Theory to Practice*, John Wiley & Sons, Inc., New York, NY, USA.

Nigdeli, S.M., Bekdas, G. and Alhan, C. (2014), "Optimization of seismic isolation systems via harmony search", *Eng. Optim.*, **46**(11), 1553-1569.

Providakis, C.P. (2008), "Effect of LRB isolators and supplemental viscous dampers on seismic isolated

buildings under near-fault excitations", *Eng. Struct.*, **30**(5), 1187-1198.

Rafiee, A., Talatahari, S. and Hadidi, A. (2013), "Optimum design of steel frames with semi-rigid connections using big bang-big crunch method", *Steel Compos. Struct.*, **14**(5), 431-451.

Roy, B.K. and Chakraborty, S. (2013), "Optimal design of base isolation system considering uncertain bounded system parameters", *Struct. Eng. Mech.*, **46**(1), 19-37.

Shi, Y. and Eberhart, R. (1998), "A modified particle swarm optimizer", *Proc. IEEE Int. Conf. Evolutionary Computation*, Piscataway, IEEE Press, 69-73.

Su, L., Ahmadi, G. and Tadjbakhsh, J.G. (1990), "A comparative study of performances of various base isolation systems, part II: sensitivity analysis", *Earthq. Eng. Struct. Dyn.*, **19**(1), 21-33.

Taflanidis, A. (2007), "Stochastic system design and applications to stochastically robust structural control", Ph.D. Dissertation, California Institute of Technology, California, USA.

Vasiliadis, L.K. (2016), "Seismic evaluation and retrofitting of reinforced concrete buildings with base isolation systems", *Earthq. Struct.*, **10**(2), 293-311.

Yamamoto, M., Minewaki, S., Higashino, M., Hamaguchi, H., Kyuke, H., Sone, T. and Yoneda, H. (2009), "Performance tests of fully size rubber bearings for isolated super high-rise buildings", *Proceedings of International Symposium on Seismic Response Controlled Buildings for Sustainable Society*, Tokyo, Japan, September.

Yamamoto, M., Minewaki, S., Yoneda, H. and Higashino, M. (2012), "Nonlinear behavior of high-damping rubber bearings under horizontal bidirectional loading: full-scale tests and analytical modeling", *Earthq. Eng. Struct. Dyn.*, **41**(13), 1845-1860.

Zhang, Y., Web, B. and Liu, Q. (1998), "First passage of uncertain single degree-of-freedom nonlinear oscillations", *Comput. Meth. Appl. Mech. Eng.*, **165**(1), 223-231.

Zou, X-K., Wang, Q., Li, G. and Chan, C-M. (2010), "Integrated reliability-based seismic drift design optimization of base-isolated concrete buildings", *J. Struct. Eng.*, ASCE, **136**(10), 1282-1295.

CC